Anomalous fluctuations in sliding motion of cytoskeletal filament driven by molecular motors: Model simulations

Yasuhiro[1] Imafuku, Namiko Mitarai[2], Katsuhisa Tawada[1], and Hiizu Nakanishi[2]

[1] *Department of Biology, Kyushu University, Fukuoka 812-8581, Japan*
[2] *Department of Physics, Kyushu University, Fukuoka 812-8581, Japan*

Abstract

It has been found in *in vitro* experiments that cytoskeletal filaments driven by molecular motors show finite diffusion in sliding motion even in the long filament limit [Y. Imafuku *et al.*, Biophys. J. 70 (1996) 878-886; N. Noda *et al.*, Biophys. 1 (2005) 45-53]. This anomalous fluctuation can be an evidence for cooperativity among the motors in action because fluctuation should be averaged out for a long filament if the action of each motor is independent. In order to understand the nature of the fluctuation in molecular motors, we perform numerical simulations and analyse velocity correlation in three existing models that are known to show some kind of cooperativity and/or large diffusion coefficient, i.e. Sekimoto-Tawada model [K. Sekimoto and K. Tawada, Phys. Rev. Lett. 75 (1995) 180], Prost model [J. Prost *et al.*, Phys. Rev. Lett. 72 (1994) 2652], and Duke model [T. Duke, Proc. Natl. Acad. Sci. USA, 96 (1999) 2770]. It is shown that Prost model and Duke model do not give a finite diffusion in the long filament limit in spite of collective action of motors. On the other hand, Sekimoto-Tawada model has been shown to give the diffusion coefficient that is independent of filament length, but it comes from the long time correlation whose time scale is proportional to filament length, and our simulations show that such a long correlation time conflicts with the experimental time scales. We conclude that none of the three models do not represent experimental findings. In order to explain the observed anomalous diffusion, we have to seek for the mechanism that should allow both the amplitude and the time scale of the velocity correlation to be independent of the filament length.

keywords: molecular motor, sliding motion, anomalous fluctuation, cooperativity, model simulation

1 Introduction

One of the outstanding problems in molecular processes in living systems has been how they achieve reliable action under the influence of overwhelming thermal and/or statistical fluctuations. In the case of muscle contraction, Huxley[1] has already noticed, in his original work, that collective action of many motors produces smooth sliding motion even though action of individual motor is highly stochastic.

Recently, Imafuku and co-workers have done series of experiments on filament motion driven by many molecular motors; Focusing on the *fluctuation* rather than the average motion, they have revealed an intriguing aspect of co-operativity in the collective action[2, 3, 4, 5].

They performed the *in vitro* motility assay on an unloaded filament of length L, measured the displacement $X(t)$ over the time interval between t_0 and $t_0 + t$, and evaluated the diffusion coefficient D in the sliding motion defined by

$$D = \lim_{t\to\infty} \frac{\left\langle (X(t) - \langle X(t)\rangle)^2 \right\rangle}{2t}, \tag{1}$$

where $\langle \cdots \rangle$ denotes the average over initial time t_0 and samples. If each motor exerting the force to the filament is statistically independent, the fluctuation is averaged out as the filament length L becomes longer, namely, as the number of motors that interact with the filament becomes larger. It has been shown that D decreases in proportion to $1/L$ for random action of independent motors[6]. In the experiments, however, they have found that D is not proportional to $1/L$ but converges to a constant value for large L. This means that the motors are not interacting with the filament independently but their actions are correlated with each other.

In order to understand these results, Sekimoto and Tawada have analyzed the motion of a cytoskeletal filament driven by protein motors with random orientation, and demonstrated that the diffusion coefficient D of its motion is independent of the filament length due to the randomness quenched in the motor orientation[7]. Later, however, Noda *et al* have found similar behavior of D even for the case where Sekimoto and Tawada model is not applicable, i.e. the case where the myosins are not random but aligned[5].

No other model has been known to show the constant D so far, and origin of the observed fluctuations has not been understood yet.

In this paper, we study fluctuations of cytoskeletal filament motion in de-

tail for three existing models: Sekimoto and Tawada model[7], Prost model[8, 9, 10, 11], and Duke model[12]; These are known to produce some kind of co-operativity[13]. As a tool to analyze dynamics, we examine *the velocity-correlation function* of the filament sliding motion obtained by numerical simulations. Nature of dynamics shows up in detailed feature of the velocity correlation function, and the diffusion coefficient can be derived from its integration.

In Sec.2, some of the basic formulas are introduced in connection with the diffusion coefficient and the velocity correlation. Detailed description and results for each model are presented with discussions for Sekimoto-Tawada model in Sec.3, for Prost model in Sec.4, and for Duke model in Sec.5. Concluding remarks are given in Sec.6.

2 Diffusion Coefficient and Velocity Correlation

Imafuku *et al.*[2, 3, 4] measured the variance of positional fluctuation of the filament defined as

$$F_r^2(t) \equiv \Big\langle (X(t) - \langle X(t) \rangle)^2 \Big\rangle, \tag{2}$$

where $X(t)$ is the displacement over the time interval of length t. The average displacement $\langle X(t) \rangle$ is linear in time, and the mean velocity V of the filament is determined by

$$V = \lim_{t \to \infty} \frac{\langle X(t) \rangle}{t}. \tag{3}$$

They found that $F_r^2(t)$ increases linearly in time. This is an ordinary diffusion process, and is characterized by the diffusion coefficient D defined by

$$D \equiv \lim_{t \to \infty} \frac{F_r^2(t)}{2t}. \tag{4}$$

In the actual experiments, it has been found that $F_r^2(t)$ behaves as

$$F_r^2(t) \approx 2Dt + \sigma, \tag{5}$$

with a constant σ, which mainly comes from the finite spatial resolution in experiments[2].

The diffusion around the average motion comes from the velocity fluctuations in the sliding motion, and $F_r^2(t)$ can be expressed as

$$F_r^2(t) = 2t \int_0^t \left(1 - \frac{s}{t}\right) C_v(s) \mathrm{d}s \tag{6}$$

in terms of the velocity correlation

$$C_v(t) = \Big\langle (v(t_0) - V)(v(t_0 + t) - V) \Big\rangle, \tag{7}$$

where $v(t)$ is the velocity at time t and V is the average velocity. The derivation of eq.(6) is given in Appendix.

Note that the relation (6) is modified when the data is only available at discrete times by the step τ as in the experiments or our Monte Carlo (MC) simulations: In this case, defining of velocity at time $t_j = \tau j$ as $v(t_j) = [X(t_j + \tau) - X(t_j)]/\tau$, the diffusion coefficient D is given by

$$D = \left[\frac{1}{2} C_v(0) + \sum_{j=1}^{\infty} C_v(t_j)\right] \tau, \tag{8}$$

in the long-time limit(see Appendix).

The velocity correlation function $C_v(t)$ goes to zero when t becomes large enough compared to any relevant correlation time, therefore, the second term contribution in eq.(6) becomes negligible in the large t limit, consequently, $F_r^2(t)$ increases linearly in time and D in eq.(4) can be expressed by

$$D = \int_0^{\infty} C_v(s) \mathrm{d}s, \tag{9}$$

namely, the diffusion coefficient is given by the integral of the velocity correlation function.

Actual measurements are always based on finite time observations, thus we define the finite time diffusion coefficient $D_{\mathrm{ft}}(t)$ as the slope of $F_r^2(t)$ at t, then we can show

$$D_{\mathrm{ft}}(t) \equiv \frac{1}{2} \frac{\mathrm{d}}{\mathrm{d}t} F_r^2(t) = \int_0^t C_v(s) \mathrm{d}s, \tag{10}$$

namely, only the correlation shorter than t contributes to $D_{\mathrm{ft}}(t)$.

Experimentally determined diffusion coefficient based on the measurement of variance for the time interval t corresponds to $D_{\mathrm{ft}}(t)$. This should

give a good approximation for the diffusion coefficient (9), if t is large enough compared to the correlation times. We should be careful about the effect of the measurement time t when we interpret the results, because we do not know the length of correlation time for the system in advance. Imafuku and coworkers estimated the diffusion coefficient D from experimental data by the slope of $F_r^2(t)$ at around $t \approx 2\,\mathrm{s}$ for microtubules driven by kinesin[3] $t \approx 0.5\,\mathrm{s}$ for microtubules driven by dynein[4], and $t \approx 0.4\,\mathrm{s}$ for actin filaments driven by myosin[5].

In the following, we analyze the diffusion constant D along with the velocity correlation.

3 Sekimoto and Tawada Model

Sekimoto and Tawada have proposed a simple model to explain dynamical fluctuations in the motion of a cytoskeletal filament driven by protein motors fixed on a substrate surface[7]; The motor proteins are assumed to be aligned at regular intervals q but in random orientation, and a filament of the length L slides over the motors in one direction in the presence of ATP. The sliding motion is generated by the motors, which are assumed to attach to the filament with the rate constant k_{b}, make a conformational change or "power stroke" to generate force, and detach from the filament with the rate constant k_{ub}. The motors interact with the filament independently. If the linear force law between the filament and the motors is employed, the sliding distance generated by a power stroke of the width a_i by the i'th motor would be a_i/N_b, where N_b is the number of the motors that attach to the filament at the time of the stroke. The factor N_b^{-1} comes from the fact that the motors bound to the filament at the time resist the sliding motion. The value of stroke width a_i for the i'th motor is always the same, but different at random from that of other motors because of its random orientation.

Sekimoto and Tawada have demonstrated that the model shows L independent diffusion constant.

3.1 Simulation method

We simulate Sekimoto-Tawada model by the following MC procedure with the time τ for one MC step: (a) Pick a motor, say i, at random out of the motors under the filament. (b) If the i'th motor is not attached to the

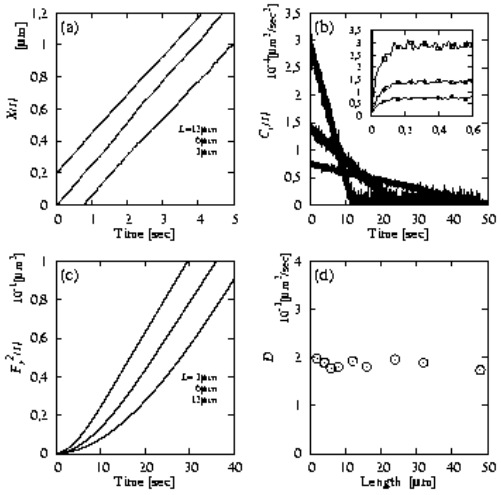

Figure 1: Sliding motion of Sekimoto-Tawada model. (a) Typical trajectories of filaments with the length L =3(bottom), 6, and 12(top) μm. The average velocity $V = 0.25\mu$m/s is independent of the filament length L. (b) Velocity correlation $C_v(t)$ for filaments with L =3, 6, and 12 μm. The inset shows short time behaviors ($0 < t \leq 0.6$ s). (c) Variance as a function of time interval for L =3(top), 6, and 12(bottom) μm. (d) Length dependence of the diffusion coefficient D measured from the slope for $L/V \leq t \leq 2L/V$.

filament, attach it with the probability $k_{\rm b}\tau$, and advance the filament by a_i/N_b. If the i'th motor is already attached to the filament, detach it with the probability $k_{\rm ub}\tau$ without any motion of the filament.

One MC step of τ corresponds to repeating this procedure N times, where N is the number of motors that are capable of attaching to the filament: $N = L/q$. The results do not depend on τ as long as $\tau k_{\rm b} \ll 1$ and $\tau k_{\rm ub} \ll 1$.

We adopt the rate constant of the motor attachment $k_{\rm b} = 6.3\,{\rm s}^{-1}$, that of the detachment $k_{\rm ub}$ =14.7 s^{-1}, and the distance between motors $q = 42.9$ nm. The width of the power stroke a_i is chosen out of random numbers with the uniform distribution ranging between 0 and 34 nm with the average 17 nm. The time step τ is taken to be 0.01 s.

3.2 Simulation results

Figure 1(a) shows typical trajectories of filaments with L =3, 6, and 12 μm. The average velocity V is 0.25μm/s, and is independent of L.

Figure 1(b) shows the velocity correlation $C_v(t)$ for rather long time ($0 < t \leq 50\,\mathrm{s}$), and the inset shows the short time behaviors for $0 < t \leq 0.6$ s. We find following characteristic behavior in $C_v(t)$: (i) At $t = 0$, the velocity correlation $C_v(0)$ is the variance of the velocity fluctuation, which takes a certain positive value. (ii) For $t > 0$, $C_v(t)$ drops immediately to almost zero, but recovers quickly to reach the maximum. (iii) After the short time recovery, $C_v(t)$ decays linearly over a long period of time. (iv) The value of $C_v(t)$ scales as to $1/L$ for both $t = 0$ and the maximum value described at (ii).

Note that the actual values of instantaneous velocity variance $C_v(0)$ do not have physical meaning because the model assumes instantaneous displacement by a stroke of molecular motor.

The immediate drop of $C_v(t)$ comes from the fact that the consecutive strokes to the filament is random. The short time recovery is due to the correlation given by the strokes from the same motors. The time T when the maximum correlation is achieved corresponds to the time interval that each motor gives successive strokes to the filament, namely $T \approx 1/k_{\mathrm{b}} + 1/k_{\mathrm{ub}} (\approx 0.23\,\mathrm{s})$. This time does not depend on L. The gradual linear decay after that comes from the loss of correlation due to the fact that new motors come into play as the filament moves. The correlation is lost completely when the filament proceeds over the distance L and resides on a new set of motors, therefore, the time scale for this correlation is L/V.

The variance of displacement $F_r^2(t)$ is shown in Fig.1(c) by a solid line for L =3, 6, and 12 μm. We see that the slope increases gradually in course of time till $t \approx L/V$. This comes from the slow decay of the velocity correlation $C_v(t)$ in Fig.1(b) through Eq.(6), namely, the slope at time t is given by the integration of $C_v(s)$ for $0 \leq s \leq t$. The slope of the variance is proportional to $1/L$ for a fixed short time $t \ll L/V$, because $C_v(t) \propto 1/L$ for a fixed time $t < L/V$. The slope for long time $t > L/V$, however, becomes independent of L, because the range that $C_v(t)$ is non-zero is proportional to L.

Fig.1(d) shows the diffusion coefficient D obtained from the slope for long time (fitted in the range $L/V \leq t \leq 2L/V$). One can see that D tends to a non-zero constant for larger L. As denoted above, however, D should be proportional to $1/L$ if one measures at fixed $t \ll L/V$ in this model.

3.3 Discussions

The key of this model is that each motor gives strokes of its inherent strength, simulating the experimental situation where motors are fixed to a substrate surface in random orientation and are not aligned to the direction of the filament; Each motor always gives the same stroke, although it varies from motor to motor. This makes the correlation time in velocity fluctuation proportional to L, and results in the L independent diffusion constant. If a stroke a_i by a motor changes randomly every time it gives a stroke, the correlation time is independent of L, thus the diffusion coefficient D would be proportional to $1/L$.

This assumption of quenched randomness in stroke in the Sekimoto-Tawada model is introduced in order to simulate the experimental situations by Imafuku *et al.*[3, 4], where microtubules are driven by motors scattered randomly on a substrate. Their results that the diffusion coefficient in sliding motion of microtubules is independent of L are reproduced by the model.

The present analysis shows, however, that this does not necessarily justify the model because the experimental time scales are not in the range where the model gives L independent diffusion coefficient. In these experiments, L/V was 0.5 s to 2 s in Ref.[3] and 0.6 s to 2.5 s in Ref.[4], while the time t of the measurement was about 2 s in Ref.[3] and 0.5 s in Ref.[4], respectively. Namely, the latter experiment by Imafuku *et al.*[4] were in the range $t < L/V$, i.e., the range where Sekimoto-Tawada model shows the diffusion coefficient that decreases with L. Therefore, the results of the model does not correspond to the experimental observation by Imafuku *et al.*[4].

Relevance of quenched randomness to the anomalous diffusion is also questionable; Kinesin has been demonstrated to swivel almost freely to adjust itself in any direction to give effective strokes[14]. Furthermore, the anomalous filament length independent diffusion has been observed even in the experiment where myosins are aligned in orientation[5].

4 Prost Model

Prost and coworkers introduced a two-state model of Brownian motor, which exhibits cooperative behavior[8, 10]. In their model, motors are attached to a backbone with a fixed spacing q, and each motor can take two states: the bound state and the unbound state. In the bound state, the motor is strongly

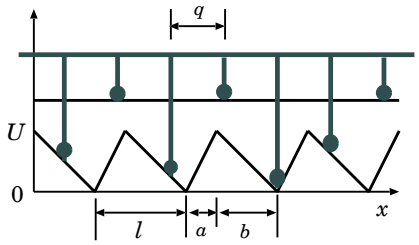

Figure 2: Prost Model

bound to a filament to exert the sliding force on it, and the interaction potential between the filament and the motor is periodic with period l along the cytoskeletal filament. A simple saw teeth potential is assumed; Each tooth of the potential height U consists of a part with a positive slope of length a and a part with a negative slope of length $b \equiv l - a$. The unbound state represents the weakly bound state, where the interaction potential is flat, and the motor does not exert force on the filament. The transition from the bound to the unbound state takes place with the rate $\omega_{\rm ub}$ only when a motor is around the potential minima within a detaching region of size δx. The transition from the unbound to the bound state, on the other hand, occurs everywhere with a constant rate $\omega_{\rm b}$. The inertia of the filament is assumed to be negligible, thus the instantaneous velocity of the filament v is determined by the balance between the total potential force from the motors $F_{\rm mot}$ and viscous force $-N\lambda v$, where N is the number of motors and λ is the viscous resistance coefficient per motor.

This model has been demonstrated to show a collective motion of smooth sliding when a number of motors are attached to a filament[11], in contrast with a Brownian motion under a periodic potential for a single motor system. If the periodic potential is asymmetric, the filament shows unidirectional motion, while bidirectional motion is observed when the potential is symmetric.

The cooperativity of the motors is evident especially in the symmetric case. In this case, there is no reason for the filament to proceed in one direction, but once the filament starts moving to one of the directions by chance, it tends to keep on moving in the same direction. This can be understood from the fact that the transition from the bound to the unbound state occurs only when the motors are around the potential minima; The motors are kicked out to the unbound state after they go down the potential slope exerting the force to the filament, therefore, there are more motors

going down the potential than those going up in the bound state. This state of directed motion may be regarded as a state with a broken symmetry due to the collective effect[11].

The direction of motion flips occasionally when the filament length is finite, and the interval between the flips gets exponentially long with the filament length. A theory analogous to the one for the phase transition in a magnetic system has been developed to describe this state.

4.1 Simulation method

One Monte Carlo step with the time τ consists of the two procedures: (a) the transition trials between the bound and the unbound states of motors, and (b) the filament advance. In the procedure (a), each of the N motors goes through the following transition trial depending upon its state: if the motor is in the bound state and it is located in one of the detaching regions of size δx around the potential minima, detach it to the unbound state with the probability $\omega_{\rm ub}\tau$. If the motor is in the unbound state, attach it to the bound state with the probability $\omega_{\rm b}\tau$. Otherwise, do nothing. After all of the motors go through the above trials, we perform the procedure (b), where the total potential force $F_{\rm mot}$ acting on the motors in the bound state is calculated, and then the filament is displaced by τv with the filament velocity $v = F_{\rm mot}/(N\lambda)$.

The period of potential is taken to be $l = 8\,{\rm nm}$, and the motor spacing $q = 42.9\,{\rm nm}$ with small random distribution of the width $\pm 0.01\,{\rm nm}$; The small distribution is introduced in order to avoid factitious interference between the motor spacing and the potential periodicity. The potential is chosen to be $a/l = 0.2$ and $U = 20k_BT$ with $k_BT = 4.14\,{\rm pN\,nm}$[9]. The transition rates are $\omega_{\rm ub}^{-1} = 2$ ms and $\omega_{\rm b}^{-1} = 25$ ms, and the size of the detaching region is $\delta x = 1.6$ nm. We also adopt the viscous resistance coefficient $\lambda = 1.29 \times 10^{-5}\,{\rm kg/s}$.

4.2 Simulation results

Examples of the simulated displacements of motors versus time under no load condition are shown for L =3, 6, and 12 μm in Fig.3(a). The average velocity is almost independent of the filament length L, but slightly smaller for shorter filaments: V =0.239, 0.248, and 0.252 μm/s for L =3, 6, and 12 μm, respectively. The detailed structure of trajectories are shown in the

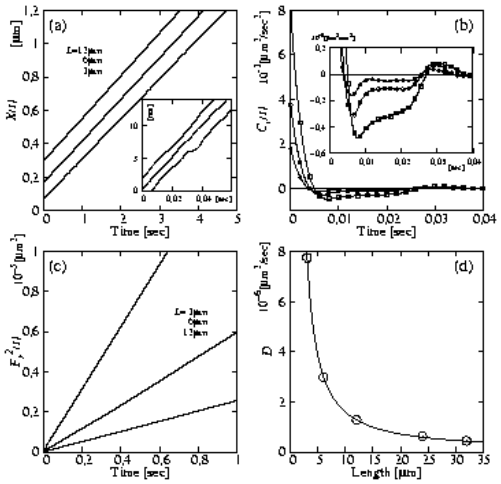

Figure 3: Sliding motion of Prost model. (a) Typical trajectories of filaments with the length L =3(bottom), 6, and 12(top) μm. The average velocity is almost independent of the filament length L, but slightly smaller for shorter filaments: V =0.239, 0.248, and 0.253 μm/s for L =3, 6, and 12 μm, respectively. (b) Velocity correlation $C_v(t)$ for filaments with L =3(open square), 6(open circle), and 12(filled circle) μm. The inset shows the behaviors for $t > 0$ s in larger scale. (c) Variance as a function of time interval for L =3(top), 6, and 12(bottom) μm. (d) Length dependence of the diffusion coefficient D. The solid line shows a fitting curve $a/L \cdot (1+b/L)$ via constants $a = 12.72 \times 10^{-6}\,\mu\mathrm{m}^3/\mathrm{s}$ and $b = 2.48\,\mu\mathrm{m}$.

inset, where one can see more fluctuations in a shorter filament. Figure 3(b) shows the velocity correlation $C_v(t)$, for which we note the following characteristics: (i) $C_v(t)$ is largest at $t = 0$, and decays rapidly to reach the negative minimum around $t \sim 6$ ms. (ii) Then, it increases gradually to reach the positive maximum at the time $t \sim 30$ ms, and decays to zero as t increases. (iii) The value of $C_v(t)$ is proportional to the inverse of the length of filament, or the number of motors. In Fig. 3(c), the variance $F_r^2(t)$'s are shown as a function of time. The diffusion coefficient is evaluated from the time dependence of the variance by fitting the data for $0\,\mathrm{s} < t < 0.8\,\mathrm{s}$ to Eq.(5). The obtained values of the diffusion coefficient D versus the length of the filament L are shown in Fig. 3(d) with a fitting curve $a/L \cdot (1 + b/L)$.

4.3 Discussions

The velocity fluctuation in this model comes from random transition of motors between the two states. Consequently, the amplitude of velocity correlation is proportional to $1/L$ for large L, reflecting the fact that the transitions of each motor is independent. The time scale of the initial decay in $C_v(t)$ is set by the transition rate ω's, and the correlation time of the positive peak in $C_v(t)$ at $t \sim 30$ ms is the time that a motor passes the period of the potential ($l/v = 8$ nm / 0.25 nm $(\mathrm{ms})^{-1} \sim 30$ ms), thus, both of the time scales are independent of L while $C_v \propto 1/L$, therefore, the resulting diffusion constant for this model is proportional to $1/L$ as is seen in Fig.3(d).

5 Duke Model

Duke[12] proposed a model for the myosin mechanochemical cycle, based on the "swinging lever arm" hypothesis, and demonstrated that the model shows collective behavior of myosins through coupling of ATP hydrolysis with conformational change of myosin head. The conformation change is amplified by a lever arm to produce a power stroke. The power stroke stretches the myosin neck and the actin filament slides as the neck relaxes.

The ATP hydrolysis cycle is simplified as in Fig.4 (a); A main stroke of the step width d takes place at the transition from $\mathrm{A \cdot M \cdot ADP \cdot Pi}$ to $\mathrm{A \cdot M \cdot ADP}$, then a small stroke of the width δ follows at the subsequent transition to $\mathrm{A \cdot M}$.

Eliminating a couple of transient states, i.e. $\mathrm{A \cdot M}$ and $\mathrm{M \cdot ATP}$, this

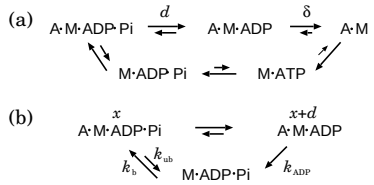

Figure 4: ATP hydrolysis cycles.

cycle is further simplified to the three-state cycle shown in Fig.4 (b), where the small step is included in the transition from $\mathrm{A}\cdot\mathrm{M}\cdot\mathrm{ADP}$ to $\mathrm{M}\cdot\mathrm{ADP}\cdot\mathrm{Pi}$.

To each myosin in the attached state $\mathrm{A}\cdot\mathrm{M}\cdot\mathrm{ADP}\cdot\mathrm{Pi}$, Duke assigned the displacement x of the neck, which becomes $x+d$ for $\mathrm{A}\cdot\mathrm{M}\cdot\mathrm{ADP}$ after a stroke. The elastic energy of the myosin neck at the state $\mathrm{A}\cdot\mathrm{M}\cdot\mathrm{ADP}\cdot\mathrm{Pi}$ and that at the state $\mathrm{A}\cdot\mathrm{M}\cdot\mathrm{ADP}$ are $Kx^2/2$ and $K(x+d)^2/2$, respectively, with the spring constant of the neck K.

The binding rate k_b from $\mathrm{M}\cdot\mathrm{ADP}\cdot\mathrm{Pi}$ to $\mathrm{A}\cdot\mathrm{M}\cdot\mathrm{ADP}\cdot\mathrm{Pi}$ with the neck displacement x is affected by this elastic energy; The binding rate to the state with the neck displacement in the range $[x, x+\mathrm{d}x]$ is given by

$$k_b\,\mathrm{d}x = k_b^0\sqrt{\frac{K}{2\pi k_B T}}\,\exp\left[-\frac{Kx^2}{2k_B T}\right]\mathrm{d}x, \tag{11}$$

while the unbinding rate k_{ub} for the opposite transition is assumed to be constant and independent of x.

The transition between the pre and post stroke states, i.e. $\mathrm{A}\cdot\mathrm{M}\cdot\mathrm{ADP}\cdot\mathrm{Pi}$ and $\mathrm{A}\cdot\mathrm{M}\cdot\mathrm{ADP}$, is fast and the population ratio is assumed to be equilibrated as the ratio of the probability distribution

$$\frac{P\left(\mathrm{A}\cdot\mathrm{M}\cdot\mathrm{ADP}\right)}{P\left(\mathrm{A}\cdot\mathrm{M}\cdot\mathrm{ADP}\cdot\mathrm{Pi}\right)} = \exp\left[-\frac{\Delta G_{\mathrm{str}}+\Delta E(x)}{k_B T}\right], \tag{12}$$

where ΔG_{str} is a change in chemical free energy and

$$\Delta E(x) \equiv \frac{1}{2}K(x+d)^2 - \frac{1}{2}Kx^2$$

is a change in elastic energy.

Within the transition from $\mathrm{A}\cdot\mathrm{M}\cdot\mathrm{ADP}$ to $\mathrm{M}\cdot\mathrm{ADP}\cdot\mathrm{Pi}$, series of transitions, including ADP release with the small step δ, ATP bind followed by actin

detachment, are involved, and its overall rate is represented as

$$k_{\rm ADP} = k^0_{\rm ADP} \exp\left[-\frac{\Delta E_\delta(x)}{k_B T}\right] \tag{13}$$

with

$$\Delta E_\delta(x) \equiv \frac{1}{2}K(x+d+\delta)^2 - \frac{1}{2}K(x+d)^2, \tag{14}$$

but the transition in the opposite direction is neglected.

The time scale for the force balance is assumed to be much shorter than the time scale for the transition between the states, thus the position of a filament is always adjusted to achieve the force balance among the molecular motors as soon as one of the motors changes its state.

Duke investigated how an ensemble of motors generates sliding motion of an actin filament against load. The model displays a transition from smooth sliding to synchronized stepwise motion as the load becomes high.

5.1 Simulation method

Suppose an actin filament of the length L is sliding straight on a substrate under load. The myosin molecules are set in array on the substrate with spacing q, thus the number of the myosins that can possibly attach is $N = L/q$.

In each MC step of the time τ, the following two procedures are iterated N times: (a) transition between attached and detached states and (b) equilibration of attached molecules. Detailed procedures are implemented as follows; (a) Transition goes by two steps. (a-1) Pick a motor at random. (a-2) If the motor is not attached to the filament, then attach it with the probability $k^0_{\rm b}\tau$ with its neck displacement x chosen at random according to the distribution (11). If the motor is attached, detach it with the probability $k_{\rm ub}\tau$ or $k_{\rm ADP}\tau$, depending upon it is in A $\cdot$ M $\cdot$ ADP $\cdot$ Pi or A $\cdot$ M $\cdot$ ADP, respectively. (b) Equilibration is achieved by repeating the following steps M times. (b-1) Move the filament to the position where the force from the motors balances with the load. (b-2) Distribute all the attached myosins according to the population ratio (12).

The procedures (a) and (b) are repeated N times in one MC step of time τ; Within (b), the procedure (b-1) and (b-2) are repeated M times to ensure that the system position is relaxed to equilibrium[15].

The parameters used in the simulations are followings: the spacing between myosin molecules is $q = 42.9$ nm, the rate constant of the motor attachment $k_{\rm b}^0 = 40\,{\rm s}^{-1}$, that of the detachment $k_{\rm ub} = 2\,{\rm s}^{-1}$ and $k_{\rm ADP}^0 = 80\,{\rm s}^{-1}$, the power stroke size $d = 11$ nm, the stiffness of myosin neck $K = 1\,{\rm pN/nm}$, the thermal energy $k_BT = 4.14$ pNnm, the free energy gain $\Delta G_{\rm str} = -16.4k_BT$, and the subsequent conformational change δ =0.5 nm. The time step τ is taken to be 0.001 s and the equilibration iteration M to be 4.

5.2 Simulation results

We show two sets of data in Fig.5: the data for the case without load (Fig.5(a1-4)) and with the load F close to stalling, i.e. F =100 pN/μm(Fig.5(b1-4)). We examine the behavior near the stalling load because cooperative operation of motors has been observed under load[12], which could result in fluctuations peculiar to the model. For each case, we present trajectories, velocity correlations, time developments of displacement variance, and the filament length dependences of diffusion constant.

Figures 5(a1) and (b1) show trajectories for filaments with L =3, 6, and 12μm. The average velocity V is almost independent of L: V =2.06, 2.11, and 2.14 μm/s without load, and V =1.98, 2.25, and 2.36 $\times 10^{-2}\mu$m/s with load. The insets show detailed structure of trajectories. One can see larger fluctuations in shorter filaments. For the cases under the load, there appear back and forth movements(the inset of Fig.5(b1)); Displacement of the movement is of the order of a stroke size d, and its time scale is determined by the reaction rates. This is a result of cooperative action of motors; With more motors attached, they produce force collectively to move forward, but detachment of some motors causes backlash, which leads to further detachment.

The velocity correlations are shown in Figs.5(a2) and (b2). For both of the cases, immediately after large positive instantaneous correlation, the correlation is negative for short time and becomes positive around $t = 0.01$ s. The initial negative correlation is due to the backlash caused by detachment after a stroke. The time scale for correlation is determined by the reaction rates and does not depend on the filament length. Note that the actual value of instantaneous correlation is not meaningful in this model as in Sekimoto-Tawada model, because filament position is shifted instantaneously during the process of equilibration.

Difference between the two cases is in the amplitude of the correlation.

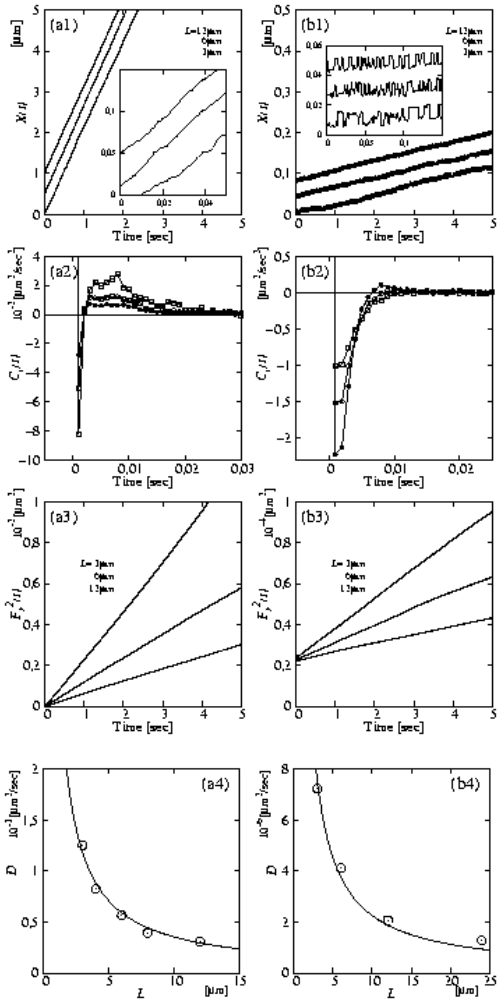

Figure 5: Sliding motion of Duke model (a1-4) for cases without load and (b1-4) with load of 100 pN/μm. (a1) and (b1) show typical trajectories of filaments with the length L =3(bottom), 6, and 12(top) μm. The average velocity V is almost independent of L: V =2.06, 2.11, and 2.14 μm/s without load, and V =1.98, 2.25, and 2.36 $\times 10^{-2}\mu$m/s with load. The insets show detailed structure of trajectories. (a2) and (b2) show the velocity correlation $C_v(t)$ for filaments with L =3(open square), 6(open circle), and 12(filled circle) μm. (a3) and (b3) show the variances as a function of time interval for L =3(top), 6, and 12(bottom) μm. (a4) and (b4) show the length dependence of the diffusion coefficient D determined by the slope of variances. The solid lines show the $1/L$ fit to the data points.

First, the amplitude is much larger for the cases with load than those without load. The large correlation in the case under load comes from the back and forth movement. Secondly, regarding the L dependence, the amplitude is larger for shorter filament for the loadless case as in the previous model, while it is smaller for shorter filament for the case with load. The larger correlation for shorter filament in the loadless case corresponds to the fact that the fluctuations in trajectories are larger for shorter filaments as has been seen in Fig.5(a1). On the other hand, the larger correlation for longer filament in the case with load corresponds to the fact that the short time back-and-forth movement is more regular in longer filament(the inset of Fig.5(b1)). The fluctuation in the time scale longer than 1 second seems to be larger in shorter filament for the case with load, but the correlation in such long time scale cannot be seen in Fig.5(b2) because of statistical errors.

The time dependences of displacement variance are shown in Figs.5(a3) and (b3), and the diffusion constant estimated from these are presented in Figs.5(a4) and (b4) with the $1/L$ curves fitted to the data. For both cases, the diffusion constant is proportional to $1/L$. This is natural for the case without load, because the time scales of $C_v(t)$ are independent of L while the value of $C_v(t)$ is proportional to $1/L$. In the case with load, the large value of the correlation does not give a large value of D; This means that the back and forth movement in short time scale does not give net motion, and the diffusion comes from the fluctuation in longer time scale, where the fluctuation is larger for shorter filament even in the case with load.

5.3 Discussions

The diffusion constant decreases as $1/L$ with the filament length L. In the case without load, the situation is simple; the time scale of velocity correlation is independent of L and its value is proportional to $1/L$, which gives $D \propto 1/L$.

In the case with load, the motors on a filament operate collectively, which results in back and forth movement in short time scale. This back and forth movement becomes more regular and gives larger value of correlation for longer filament, but does not results in larger diffusion. The diffusion in the sliding motion comes from longer time fluctuations, which is larger for shorter filament.

6 Concluding Remarks

Our results of numerical simulations are summarized as follows: (i) Although the amplitude of velocity correlation function decreases as $1/L$, Sekimoto-Tawada model shows the L independent diffusion coefficient D because the time scale of velocity correlation is given by L/V, thus proportional to L. (ii) Prost model shows $D \propto 1/L$ because the amplitude of velocity correlation is proportional to $1/L$ and its time scale is independent of L. (iii) Duke model also shows $D \propto 1/L$ as in Prost model.

Although the anomalous diffusion in the experiments is observed without load, we examined Duke model with load also, because Duke model has been denmonstrated to show a synchronous operation under load and we expected that filament motion caused by collective operation of motors was a possible explanation for large diffusion. However, the collective movement by synchronous operation under load in Duke model did not turn out to produce large diffusion for a long filament; It gives rather regular back and forth movement in short time, but did not give a net motion for longer time.

In connection with the experimental observation that D is finite in the large L limit, the L independent D in Sekimoto-Tawada model is not likely to be relevant; In the experimentally determination of diffusion coefficient, only the time dependences of the variance shorter than a few seconds are used, which means that the velocity correlation shorter than a few seconds is relevant, while the correlation time in Sekimoto-Tawada model is of order of L/V, which can be much longer than the experimental time scale for a long filament.

In conclusion, by examining the velocity correlation and the diffusion coefficient, we have confirmed the existing models cannot account for the anomalous fluctuation that the diffusion coefficient remains finite even in the large L region. Our analysis shows that the experimental observations of L-independent diffusion coefficient require a mechanism that makes both the amplitude and the time scale of velocity correlation function independent of L.

A Relation between Variance and Velocity correlation Function

We briefly summarize the derivation for some formulas which express the variance $F_r^2(t)$ in terms of the velocity correlation function $C_v(t)$ following Ref.[16] for both the continuous and discrete time data.

A.1 Continuous time expression

The position of the filament $X(t)$ at time t is given by

$$X(t) = X(0) + \int_0^t v(t)\mathrm{d}t, \tag{15}$$

and the average position becomes

$$\langle X(t) \rangle = X(0) + \int_0^t V\mathrm{d}t. \tag{16}$$

Thus, the variance (2) is given by

$$\begin{aligned} F_r^2(t) &= \int_0^t \mathrm{d}t' \int_0^t \mathrm{d}t'' \langle (v(t') - V)(v(t'') - V) \rangle \\ &= 2\int_0^t \mathrm{d}t' \int_0^{t'} \mathrm{d}t'' C_v(t' - t''). \end{aligned} \tag{17}$$

Here, we assumed that the velocity correlation $C_v(t) = \langle (v(t_0) - V)(v(t_0 + t) - V) \rangle$ is the function of t and does not depend on t_0.

If we take new variables $s = t' - t''$ and $s' = t'$, the integration (17) becomes

$$\begin{aligned} F_r^2(t) &= 2\int_0^t \mathrm{d}s' \int_0^{s'} \mathrm{d}s C_v(s) \\ &= 2\left(\left[s' \int_0^{s'} \mathrm{d}s C_v(s) \right]_{s'=0}^{s'=t} - \int_0^t \mathrm{d}s' s' C_v(s') \right) \\ &= 2t \int_0^t \left(1 - \frac{s}{t} \right) C_v(s)\mathrm{d}s, \end{aligned} \tag{18}$$

where we have performed the partial integration.

A.2 Discrete time expression

For the data at the discrete time sequence $t_j = j\tau$ $(j = 0, 1, 2, \cdots)$, we define the velocity fluctuation as $\tilde{v}_j \equiv v_j - V$. The position at time t_n is given by $x_n = \sum_{i=1}^{n} v_i \tau$, and its average is given by $\langle x_n \rangle = Vn\tau$. Thus we have

$$\begin{aligned}
\left\langle (x_n - \langle x_n \rangle)^2 \right\rangle &= \left\langle \sum_{i=1}^{n} \tilde{v}_i \sum_{j=1}^{n} \tilde{v}_j \right\rangle \tau^2 \\
&= \left\langle \sum_{i=1}^{n} \tilde{v}_i^2 + \sum_{i=2}^{n} \sum_{j=1}^{i-1} \tilde{v}_i \tilde{v}_j + \sum_{j=2}^{n} \sum_{i=1}^{j-1} \tilde{v}_i \tilde{v}_j \right\rangle \tau^2 \\
&= 2 \sum_{i=2}^{n} \sum_{j=1}^{i-1} \langle \tilde{v}_i \tilde{v}_j \rangle \tau^2 + \sum_{i=1}^{n} \langle \tilde{v}_i^2 \rangle \tau^2 \qquad (19)
\end{aligned}$$

Now, we assume that $C_v(t_i, t_j) = \langle \tilde{v}_i \tilde{v}_j \rangle$ depends only on $|t_i - t_j|$, namely, $C_v(t_i, t_j) = C_v(|t_i - t_j|)$. Then, the first term in (19) becomes

$$\begin{aligned}
\sum_{i=2}^{n} \sum_{j=1}^{i-1} C_v(t_i, t_j) &= \sum_{i=2}^{n} \sum_{k=1}^{i-1} C_v(t_k) \\
&= \sum_{k=1}^{n-1} \sum_{i=k+1}^{n} C_v(t_k) = \sum_{k=1}^{n-1} (n-k) C_v(t_k) \qquad (20)
\end{aligned}$$

while we have $\sum_{i=1}^{n} \langle \tilde{v}_i^2 \rangle = nC(0)$ for the second term in (19). Therefore, in the large t_k limit, we have from Eqs.(19) and (20) with the definition (4) that

$$D = \left[\frac{C(0)}{2} + \sum_{k=1}^{\infty} C(t_k) \right] \tau, \qquad (21)$$

which is eq. (8).

References

[1] Huxley, A. *Prog. Biophys. Biophys. Chem.* **1957**, *7*, 255–318.

[2] Imafuku, Y.; Toyoshima, Y.; Tawada, K. *Biophys. Chem.* **1996**, *59*, 139–153.

[3] Imafuku, Y.; Toyoshima, Y.; Tawada, K. *Biophys. J.* **1996**, *70*, 878–886.

[4] Imafuku, Y.; Toyoshima, Y.; Tawada, K. *Biophys. Chem.* **1997**, *67*, 117–125.

[5] Noda, N.; Imafuku, Y.; Yamada, A.; Tawada, K. *Biophysics* **2005**, *1*, 45–53.

[6] Sekimoto, K.; Tawada, K. *Biophys. Chem.* **2001**, *89*, 95–99.

[7] Sekimoto, K.; Tawada, K. *Phys. Rev. Lett.* **1995**, *75*, 180–183.

[8] Prost, J.; Chauwin, J.-F.; Peliti, L.; Ajdari, A. *Phys. Rev. Lett.* **1994**, *72*, 2652–2655.

[9] Jülicher, F.; Prost, J. *Phys. Rev. Lett.* **1995**, *75*, 2618–2621.

[10] Jülicher, F.; Ajdari, A.; Prost, J. *Rev. Mod. Phys.* **1997**, *69*, 1269–1282.

[11] Badoual, M.; Jülicher, F.; Prost, J. *Proc. Natl. Acad. Sci. USA* **2002**, *99*, 6696–6701.

[12] Duke, T. *Proc. Natl. Acad. Sci. USA* **1999**, *96*, 2770–2775.

[13] Vermeulen, K.; Stienen, G.; Schmidt, C. *J. Muscle Res. Cell Motil.* **2002**, *23*, 71–79.

[14] Hunt, A.; Howard, J. *Proc. Natl. Acad. Sci. USA* **1993**, *90*, 11653–11657.

[15] The present procedure is slightly different from that by Duke in his original paper; Duke employed only the redistribution of population in the equilibration process, while we include a filament displacement in equilibration in accordance with the assumption that the time to achieve the force balance is fast in comparison with the MC step.

[16] Hansen, J.; MacDonald, I. In *Theory of Simple Liquids;* Academic Press, London, 1986; chapter 7; Second ed.